Influence of the External Scale Cracking on the Ti_3Al-Based Alloy Oxidation Kinetics

Ivana Cvijović[a], Milan T. Jovanović[b]

Institute of Nuclear Sciences „Vinča“, P.O. Box 522, 11001 Belgrade, Serbia

[a]ivanac@vin.bg.ac.yu, [b]miljov@vin.bg.ac.yu

Keywords: Ti_3Al alloy, Cyclic oxidation, Ni-Cr coating, Kinetic model, External scale cracking, SEM, XRD

Abstract. The influence of external scale cracking on the cyclic oxidation kinetics of a Ti_3Al-based alloy with the composition Ti-24Al-11Nb (at.%) was studied in air at 600 and 900°C. The oxidation products formed on the alloy surface with and without a Ni-20Cr (at.%) protective coating were characterized by scanning electron microscopy (SEM) and X-ray diffraction (XRD). Oxidation kinetics was monitored up to 120 h by recording the mass gain *vs.* time data. It was found that the scales formed at both temperatures were predominantly composed of TiO_2, while Al_2O_3 was also present as a minor constituent. The scale morphology and formation rate changed with temperature. The external scale cracking and layers detachment cause the much faster oxidation kinetics at 900°C. The mass gain curves followed the linear rate low, indicating that the oxide scale is not protective in respect of oxidation. The deposited coating promotes the growth of Al_2O_3-rich protective oxides and makes the scale more compact, reducing the overall oxidation process.

Introduction

Intermetallic Ti-Al alloys, such as Ti_3Al-based alloys, are promising materials for high-temperature applications since these materials have low densities and good high-temperature mechanical properties. However, poor room-temperature ductility and oxidation resistance of binary titanium aluminides was of prime importance when development of Ti-Al alloys is concerned during last few decades and has been greatly improved by additional alloying with Nb, V and Mo [1].

Beneficial effect of additional alloying of Ti_3Al-based alloys with Nb was already reported in the literature [2]. Namely, since external scales formed during oxidation of Ti_3Al-based alloys are primary consisted of porous TiO_2 scales or TiO_2 and Al_2O_3 mixtures rater than compact Al_2O_3 protective scales, benefficial effect of Nb addition has been associated with decrease of oxygen diffusion rate throughout the externaly formed oxide scales caused with reduction of point defects present in external titanium oxide. Also, according to the available literature data [3] values of oxidation rate constant decreased with increase of the Nb content in the intermetallic alloy, but it becomes independent on Nb addition greater than 10 at.%.

However, additional alloying of titanium aluminides is not the only procedure which could lead to the improvement of the oxidation resistance. Since alloying with ternary elements is not sufficient to ensure a protective oxide formation, deposition of protective coatings on the alloy surface is the most promising approach to provide good oxidation resistance at high temperatures [4,5].

Therefore, the aim of present study is to examine the high-temperature oxidation behavior of Ti_3Al-based alloy as well as oxidation reactions in the alloy surface regions during exposure to air at elevated temperatures. The effect of protective coating deposition and external scale cracking on the oxidation kinetics of the Ti_3Al-based alloy was also systematically studied.

Experimental Procedures

The investigated Ti_3Al-based alloy with the composition Ti-24Al-11Nb (at.%) was supplied in the form of 0.5 mm thick hot-rolled sheets. The hot-rolling was performed at a temperature in the $(\alpha_2+\beta)$-phase field (1050°C). From the sheets, samples of 15x15 mm^2 in size were cut and metallographically prepared using SiC grounding papers. After grounding down to 1000 grit

samples were ultrasonically cleaned with ethyl alcohol for 30 min in order to free sample surfaces from contamination. One group of samples was afterwards coated with 1 μm thick Ni-20Cr (at.%) protective film using ion sputtering technique.

High-temperature cyclic oxidation was performed in air at 600 and 900°C for 120 h in five successive cycles. For oxidation cycle the samples were oxidized for 24 h at test temperature and then were furnace-cooled down to the room temperature. After each cycle mass gain was measured using the Mettler electronic balance with ±0.0001 g accuracy.

A Simens D500 PC automatic diffractometer (XRD) with CuK_α radiation was used for oxides scales determination. A JEOL JSM-6460LV scanning electron microscope (SEM) was also used to confirm the presence and the location of the major oxides observed by XRD. For this purpose, oxidized samples were cross sectioned and polished. The oxide scale thickness, morphology and composition were estimated. The elemental composition of oxidized samples was determined as a function of external scale depth by energy dispersive spectrometry (EDS) analysis conducted with an Oxford Instruments INCA X-sight system attached to the SEM.

Results and Discusion

During cyclic high-temperature treatment in air the progresive oxidation takes place. In order to define and better understand the oxidation process, the oxidation kinetic model and oxidation products must be determined.

Oxidation kinetics. There are different kinetic models to define oxidation rate. However, for kinetic model definition it is necesary to design thermogravimetric curves, which will represent the variation of the mass gain with time, as well as to determine kinetic parameters such as rate constant, oxidation rate power exponent and activation energy. Oxidation rate can be described with the basic model, following the equation:

$$(\Delta m)^n = k_p \cdot t \,. \tag{1}$$

where Δm represents the mass gain per unit surface area, n is the oxidation rate power exponent, k_p is the oxidation rate constant, while t is the oxidation time. The logarithm of Eq. 1 yields:

$$\log(\Delta m) = \frac{1}{n}\log k_p + \frac{1}{n}\log t \,. \tag{2}$$

The oxidation power exponent and oxidation rate constant can be evaluated from linear regression fitting of *log (Δm) vs. log t* data for each experiment. It must be noticed that when n equals 1 than variation of the oxidation mass gain with time is linear, when n equals 2 than *Δm vs. t* is parabolic and so on [6].

Isothermal curves shown in Fig. 1a represent mass gain data recorded after high-temperature cyclic oxidation of Ti-24Al-11Nb alloy with and without Ni-20Cr protective coating. It can be noticed that investigated alloy shows better oxidation resistance during the annealing at 600°C, disregarding the coating deposition. Namely, mass gain after 120 h long annealing of the Ti_3Al-based alloy without protective coating at 600°C is only 0.015 g/cm^2 and nearly the same value is obtained for the sample with deposited protective coating annealed at the same temperature. However, during the annealing at higher temperature mass gain rapidly increases with prolonging of the oxidation duration and for the samples without Ni-20Cr coating recorded mass gain after 120 h long annealing was 0.601 g/cm^2. Protective coating deposition slowed down oxidation process and after last oxidation cycle at 900°C mass gain of 0.486 g/cm^2 was detected.

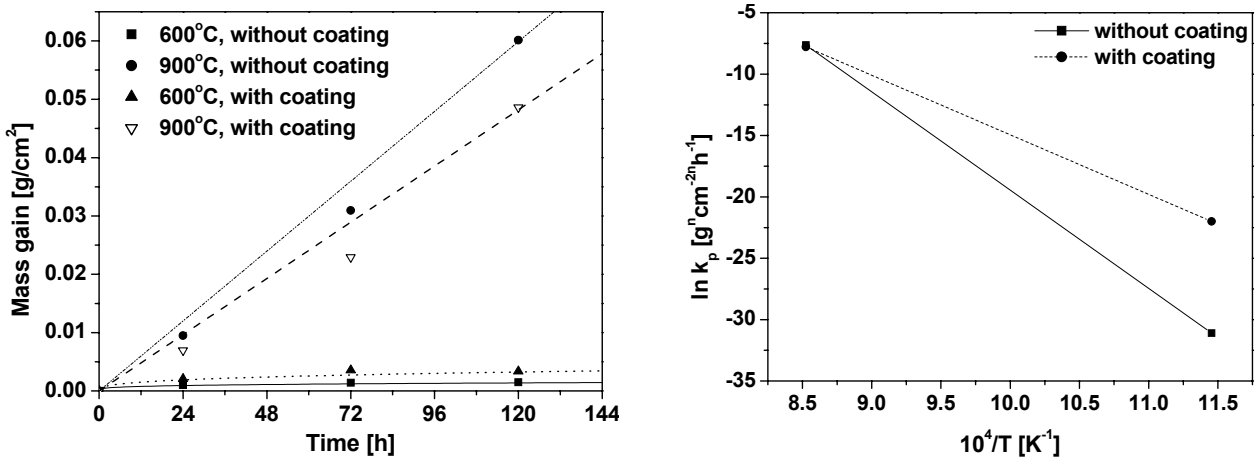

(a) (b)

Fig. 1. (a) Mass gain data and (b) Arrhenius plots of oxidation rate constants of Ti-24Al-11Nb alloy with and without Ni-20Cr protective coating.

Considering the *Δm vs. t* results previously published in the literature it was noticed that parabolic kinetic curves were mainly used for experimental data interpretation [7-9]. Because of that parabolic kinetic model was also considered for collected mass gain data interpretation during this investigation. However, parabolic model can be applied only in some cases. According to the Wagner's theory [6], oxidation rate is controlled by solid state diffusion of the reactants through a growing compact external scale. Since oxidation rate at high temperatures can be controlled by various factors (*e.g.* annealing temperature, gas atmosphere composition, external scale porousness, adherence, cracking and composition) [7,8], parabolic oxidation rate can be attained only approximately.

Results obtained in this study showed great deviation from the parabolic oxidation low, since obtained *n* values are in the range from 0.83 to 0.87 for the samples oxidized at 900°C and from 3.36 to 4.21 range for the samples annealed at 600°C with and without deposited coating, respectively.

Therefore, it was determined that oxidation data of the sample without protective coating treated at 600°C can be fitted to the following equation:

$$(\Delta m)^4 = 2{,}98419 \cdot 10^{-14} \cdot t\,. \tag{3}$$

while cubic kinetic model corresponds to the mass gain data colected during cyclic oxidation of the sample with Ni-20Cr coating annealed at the same temperature:

$$(\Delta m)^3 = 2{,}82757 \cdot 10^{-10} \cdot t\,. \tag{4}$$

On the other hand, linear oxidation rate models for samples annealed at 900°C with and without deposited coating are given, respectively, as follows:

$$(\Delta m) = 4{,}99147 \cdot 10^{-4} \cdot t\,. \tag{5}$$

$$(\Delta m) = 4{,}01603 \cdot 10^{-4} \cdot t\,. \tag{6}$$

Oxidation rate constant k_p dependence on the oxidation temperature follows Arrhenius law:

$$k_p = k_o \exp\left(-\frac{E_a}{RT}\right). \tag{7}$$

where k_o represents pre-exponential factor, E_a is the activation energy, R is the universal gas constant, while T is temperature of exposure (in K). However, in order to completely define rate constant k_p values of E_a and k_o must be determined by plotting *ln* k_p *vs. 1/T*. Figure 1b presents plots of *ln* k_p as a function of *1/T* for oxidation of samples with and without coating. The slopes of the linear best-fit lines of data points provided the values of E_a. Table 1 lists the experimentally obtained E_a and pre-exponential constant (k_o) values.

Table 1. Kinetic parameters of Ti-24Al-11Nb alloy oxidation.

Ti-24Al-11Nb alloy	***E_a [KJ/mol]***	***k_o [$g^n cm^{-2n} h^{-1}$]****
without protective coating	668.0951	$2.80755 \cdot 10^{26}$
with Ni-20Cr coating	402.0557	$3.21539 \cdot 10^{14}$

*n = oxidation rate power exponent

From the difference in the experimentaly obtained E_a values it can be concluded that oxidation process is not controlled by the same mechanisam when cyclic oxidation of the investigated Ti_3Al-based alloy with and without Ni-20Cr protective coating is concerned. Namely, linear kinetic curves point out that during cyclic oxidation protective oxide scale was not formed at the alloy surface and that some other mechanism, such as external porous scale formation, is responsable for the progress of the oxidation process [6]. Also, the obtained k_p values indicate that deposition of the protective coating did not improve oxidation resistance of the alloy during cyclic oxidation at 600°C even though oxidation process is turn out to be slow in both cases. Significant increase in the k_p values showed that alloy oxidation resistance was drasticaly reduced during exposure to air at 900°C. However, since oxidation rate is proved to be highly dependent on the surface state of the alloy it was found that deposition of the Ni-20Cr coating on the alloy surface improved its oxidation resistance, which was confirmed with obtained k_p values.

Oxide scale composition and morphology. As discussed above, the reason for these variations may be attributed to the variation in the nature and/or characteristics of scale with progress of oxidation at different temperatures. The cross-section SEM micrographs shown in Fig. 2 provide some insight into the morphological features of oxide scale.

The scales formed at 600°C were mono-layered with internal oxygen dissolution zone in the underlying substrate (Figs. 2a and b). They seem very compact, free from macroscopic defects and porosity in both cases (Figs. 2a and b). The main difference between the external scales formed on the uncoated and coated samples is their thickness and adherence. Thus, the thickness of poorly adherent scale observed on the surface of uncoated samples was found to be about 5 μm. It contains some cracks probably generated by the relief of stress present in the scale (Fig. 2a). Due to the lower oxidation rate in coated samples, a thin 2.5 μm scale was formed after 120 h (Fig. 2b). The scales were adherent and more uniform compared to those on the uncoated samples. This indicates that the chemical structure of the scales were different.

Both of the SEM/EDS and XRD analysis showed that the scale on the uncoated samples primarily consisted of TiO_2 and AlN and a minor amount of complex Ti_2AlN (Fig. 3a). The outermost layer was TiO_2, while two different nitride layers were identified beneath it. The presence of a thin nitride layer adjacent to substrate surface is possible if low partial pressure ratio (p_{O2}/p_{N2}) is achieved in the gas atmosphere. In some extent, the nitride layers represent diffusion barrier and prevent further sample degradation. In contrast, TiO_2 could not be detected in the scale formed on the coated samples. The XRD pattern revealed that a very dense and continuous layer completely composed of a stable protective Cr_2O_3 oxide. Diffraction peaks which correspond to the Ni originate from Ni-20Cr protective coating. Also, Ti_2AlN detected by the XRD was the only nitride present in the scale.

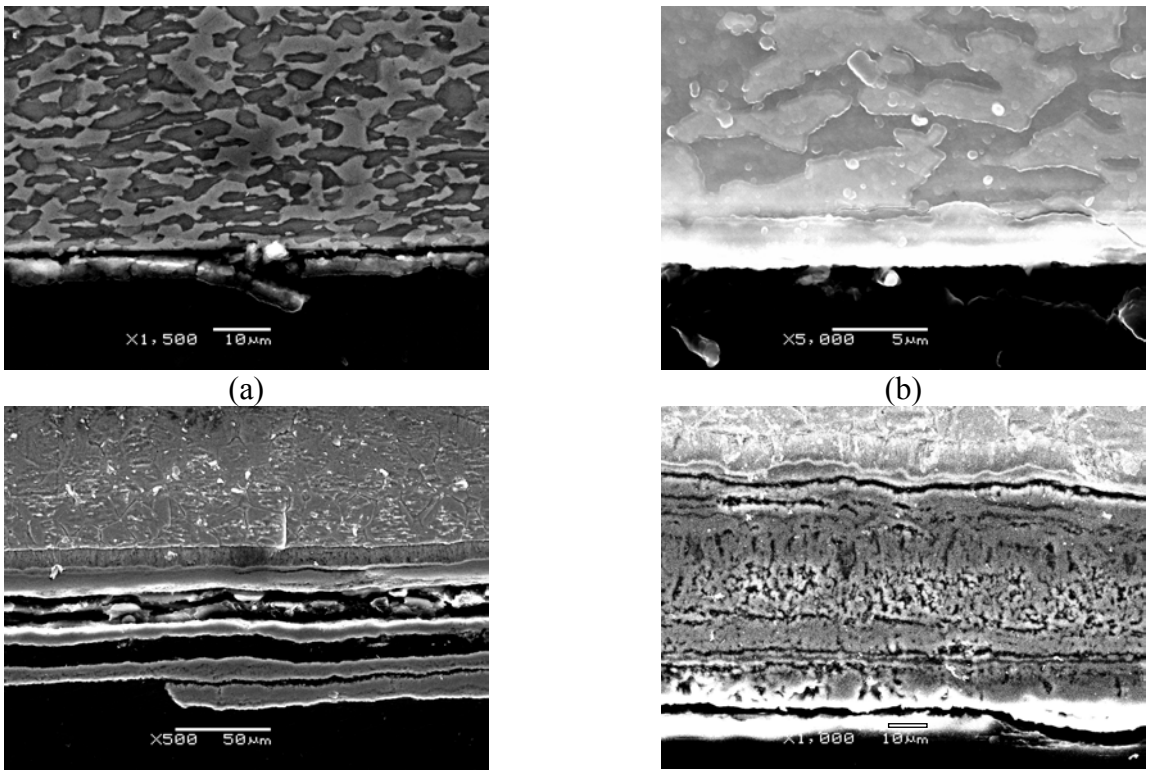

(a) (b)

(c) (d)

Fig. 2. SEM micrographs showing cross-section of the Ti-24Al-11Nb alloy without (a), (c) and (b), (d) with Ni-20Cr protective coating annealed at 600°C (a), (b) and at 900°C (c), (d) in air.

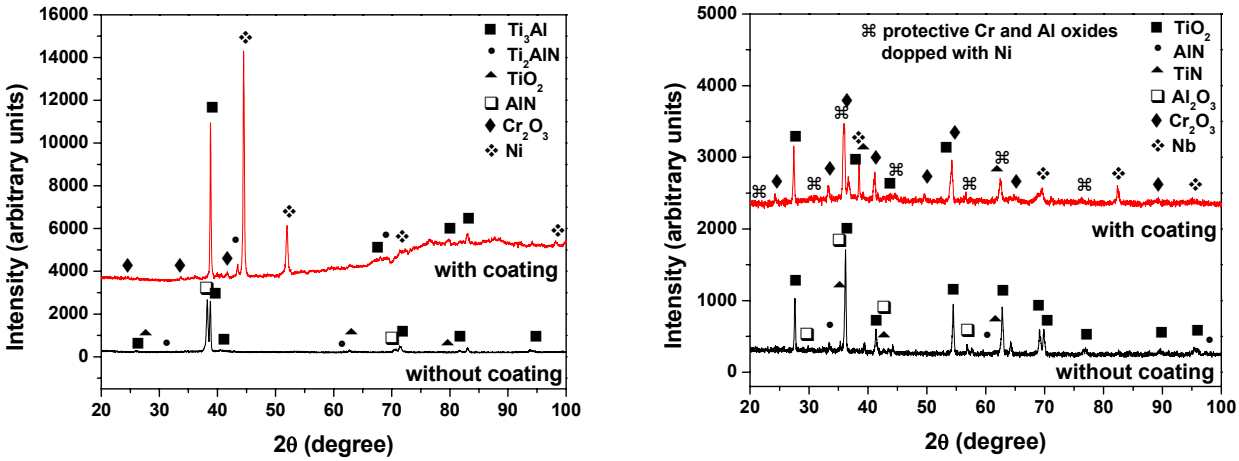

(a) (b)

Fig. 3. XRD patterns of Ti-24Al-11Nb alloy with and without Ni-20Cr protective coating annealed at (a) 600°C and (b) 900°C in air.

With the increase of oxidation temperature the oxide scale morphology and nature drastically changed. After 120 h at 900°C, the scales are very thick and multi-layerd (Figs. 2c and 2d). Such structure of scale formed *in-situ* with alternate layers of phases is more pronounced in the case of uncoated samples. Although the individual layer thickness is smaller, more layers are formed contributing to the overall 54.4 – 63.3 µm thickness of external scale. Due to the numerous interfaces, the detachment and cracking of the oxide layers took place during cooling of the samples. Cracking of the layers even more intensified gas corrosion degradation of the Ti_3Al-based alloy. The SEM/EDS analysis and XRD results, as shown in Fig. 3b, revealed that the scale is composed of TiO_2 as the major oxide and a porous layer of the TiO_2+Al_2O_3 mixed oxides in which the Nb is dissolved. At the interface between the external scale and the substrate, nitrogen enrichment and formation of narrow AlN and TiN layers were detected. Underneath this zone, internal layer with the Al_2O_3 platelets was observed (Fig. 2c).

According to observed k_p values, the presence of protective coating on the surface improves the alloy oxidation resistance at 900°C. As can be seen from Fig. 2d, the scales formed on the coated samples are thinner compared to those on the uncoated samples. The continuous Cr_2O_3 layer formed in outer part of external scale and Ni incorporation in its inner part are proved to be effective in decreasing the oxidation rate even though the porous TiO_2 is the main oxidation product (Fig. 3b). Beneficial effect of Ni-20Cr coating deposition is also reflected in protective Al_2O_3, AlN and TiN external formation along with appearance of internal Al_2O_3 layer. It is interesting to note that although the adhesion of the scale to the substrate is poor, the spallation of external scale does not take place.

Conclusions

During high-temperature cyclic annealing of Ti-24Al-11Nb alloy external and internal oxidation occurs. The scales formed at 600 and 900°C in air are mainly composed of TiO_2, while TiO_2+Al_2O_3 mixed oxides and protective nitrides are present in smaller amounts. The oxidation kinetics, nature and morphology of oxide scales change with temperature. Scales formed at lower temperature are compact and adherent, while the oxidation rate can be described with kinetic equations of fourth and third order. At higher temperature, the multi-layered scales are generally porous and loosely adherent. Due to the external scale cracking and spallation, the oxidation kinetics are much faster and linear rate low is obeyed. The Ni-20Cr coating deposition improved oxidation resistance, promoting the formation of protective Cr_2O_3 oxide and incorporation of Ni ions in porous external scales. The effect is more pronounced at higher temperature.

Acknowledgments

This research was financially supported by the Ministry of Science and Environmental Protection of the Republic of Serbia through the Project No. 144027.

References

[1] J.C. Schaeffer: Scripta Metall. Vol. 28 (1993), p. 791

[2] J. Subrahmanyam: J. Materials Science Vol. 23 (1988), p. 1906

[3] G. Qiu, J. Wu, L. Zhang and D. Lin: Scripta Metall. Mater. Vol. 33 (1995), p. 213

[4] T. Nishimoto, T. Izumi, S. Hayashi and T. Narita: Intermetallics Vol. 11 (2003), p. 459

[5] Z. Li, W. Gao and Y. He: Scripta Mater. 45 (2001), p. 1099

[6] A. Tomasi and S. Gialanella: Thermochemica Acta Vol. 269-270 (1995), p. 133

[7] T.K. Roy, R. Balasubramaniam and A. Ghosh: Metall. Mater. Trans. A Vol. 27A (1996), p. 3993

[8] T.K. Roy, R. Balasubramaniam and A. Ghosh: Metall. Mater. Trans. A Vol. 27 (1996), p. 4003

[9] M.N. Mungole, R. Balasubramaniam and A. Ghosh: Intermetallics Vol. 8 (2000), p. 717